

Density fingerprint of giant vortices in Fermi gases near a Feshbach resonance

Hui Hu^{1,2} and Xia-Ji Liu²

¹ *Department of Physics, Renmin University of China, Beijing 100872, China*
² *ARC Centre of Excellence for Quantum-Atom Optics, Department of Physics,
University of Queensland, Brisbane, Queensland 4072, Australia*

(Dated: June 8, 2018)

The structure of multiply quantized or giant vortex states in atomic Fermi gases across a Feshbach resonance is studied within the context of self-consistent Bogoliubov-de Gennes theory. The particle density profile of vortices with $\kappa > 1$ flux quanta is calculated. Owing to κ discrete branches of vortex core bound states, inside the core the density oscillates as a function of the distance from the vortex line and displays a non-monotonic dependence on the interaction strengths, in marked contrast to the singly quantized case, in which the density depletes monotonically. This feature, never reported so far, can make a direct visualization of the giant vortices in atomic Fermi gases.

PACS numbers: 03.75.Hh, 03.75.Ss, 05.30.Fk

One of the hallmarks of superfluidity of quantum fluids, be it fermionic or bosonic, is the appearance of quantized vortices. In condensed matter physics, the vortex states have been studied widely in various systems, ranging from the conventional Bardeen-Cooper-Schrieffer (BCS) superconductors to the rotating helium superfluids. The recent manipulated ultracold atomic ⁶Li and ⁴⁰K gases emerge as a new promising test-bed for the vortex physics [1]. Their interactions can be arbitrarily and precisely enhanced using a Feshbach resonance. Upon sweeping a magnetic field downward through the resonance, these Fermi systems undergo a smooth crossover from the BCS superfluidity to the Bose-Einstein condensation (BEC) of tightly bound pairs [1]. As the underlying statistics of systems changes from fermionic to bosonic across the resonance, it is interesting to ask how the properties of vortices evolve around the crossover.

A singly quantized vortex in the BCS-BEC crossover has been discussed to a certain extent [2, 3, 4, 5, 6, 7, 8, 9]. The presence of strong interactions is shown to lead to a significant depletion of the particle density in the region of the vortex core [2, 5], which was indeed confirmed experimentally by Zwierlein *et al.* for a ⁶Li gas [1]. The properties of giant vortex states with multiple flux quanta [10, 11, 12], on the other hand, is less known. Generically, in a bulk system giant vortices are not energetically favorable and are not expected to persist if created. In the confined geometry, however, the situation may be different. A number of methods have been proposed to overcome this vortex dissociation instability, including the use of an external repulsive pinning potential [13] or a trapping potential steeper than the harmonic traps [14]. As a counterpart, the giant vortex structures have been recently produced in rapid rotating trapped BECs [15]. They have also been observed in the nanoscale superconductors where the sample size becomes comparable to the superconducting coherence length ξ [16].

Given all the recent advances in experimental tech-

niques, in this paper we discuss the evolution of the giant vortex structure from weak-to-strong coupling superfluidity in trapped Fermi gases across a broad Feshbach resonance. In marked contrast to the singly quantized vortex, we find a non-trivial oscillation behavior in the particle density profile of giant vortices inside the core in the strongly interacting BCS-BEC crossover regime. The oscillation pattern, unique to the number of flux quanta at particular couplings, relates directly to the microscopic electronic spectrum of the local density of states (LDOS), which acquires an intriguing structure owing to the multiple branches of vortex core bound states, the so-called Caroli-de Gennes-Matricon (CdGM) states [17]. In this respect, it provides a density *fingerprint* for giant vortices in the neutral Fermi gases. Towards the deep BEC limit, these oscillation patterns cease to exist, and finally the density profile returns back to that of a BEC. Our results are obtained by numerically solving the Bogoliubov-de Gennes (BdG) equations in a fully self-consistent fashion. As the strongly interacting Fermi systems can be found also in various fields of physics, such as the high-temperature superconductors and neutron stars, our results can have implications beyond the cold atom physics.

To be concrete, we consider a two-dimensional (2D) Fermi gas that can be prepared readily in a single ‘pancake’ trap or at the nodes of 1D optical lattice potentials. It is sufficient to model the broad Feshbach resonance using a single channel Hamiltonian [18]. We therefore assume a 2D contact interaction parameterized by a coupling constant g . The two-body interaction problem under this circumstance involves two length scales: the characteristic length in the tightly confined direction a_0 and the 3D s -wave scattering length a_{sc} . A peculiar 2D bound state of two atoms appears for an *arbitrarily* weak attraction [19], with the binding energy $E_a/(\hbar\omega_0) = 0.915/\pi \exp(-\sqrt{2\pi}a_0/a_{sc}) \ll 1$, where $\omega_0 = \hbar/(ma_0^2)$. The bare coupling constant can then be

regularized via the s -wave scattering phase shift [20], *i.e.*,

$$\frac{1}{g} + \sum_{\mathbf{k}} \frac{1}{\hbar^2 \mathbf{k}^2 / m + E} = \frac{m}{4\pi \hbar^2} \ln \left(\frac{E_a}{E} \right), \quad (1)$$

where the relative collision energy E is of the order of the Fermi energy E_F and drops automatically out of the final results. For a uniform gas at zero temperature, the mean-field theory of the BCS-BEC crossover in 2D admits simple analytic expressions for the order parameter and chemical potential: $\Delta = (2E_F E_a)^{1/2}$ and $\mu = E_F - E_a/2$, respectively [20]. Hence, $E_a \ll E_F$ corresponds to the weak coupling BCS limit, while in the opposite BEC limit of very strong attractions, $E_a \gg E_F$. The crossover occurs approximately at $E_a \simeq 0.5E_F$ [21].

In BdG approach the quasiparticle wave functions u_η and v_η are determined by the coupled equations [22],

$$\begin{bmatrix} \mathcal{H}_0 & \Delta(\mathbf{r}) \\ \Delta^*(\mathbf{r}) & -\mathcal{H}_0 \end{bmatrix} \begin{bmatrix} u_\eta(\mathbf{r}) \\ v_\eta(\mathbf{r}) \end{bmatrix} = E_\eta \begin{bmatrix} u_\eta(\mathbf{r}) \\ v_\eta(\mathbf{r}) \end{bmatrix}, \quad (2)$$

where E_η is the excitation energy, and the single particle Hamiltonian in traps is $\mathcal{H}_0 = -\hbar^2 \nabla^2 / 2m + m\omega^2 r^2 / 2 - \mu$. As the BdG equations are invariant under the replacement $u_\eta(\mathbf{r}) \rightarrow v_\eta^*(\mathbf{r})$, $v_\eta(\mathbf{r}) \rightarrow -u_\eta^*(\mathbf{r})$, $E_\eta \rightarrow -E_\eta$, we restrict our calculations to $E_\eta \geq 0$ only. The order parameter $\Delta(\mathbf{r})$ and the chemical potential μ are determined respectively by the self-consistency equation $\Delta(\mathbf{r}) = g \sum_\eta u_\eta(\mathbf{r}) v_\eta^*(\mathbf{r}) [1 - 2f(E_\eta)]$ and the particle density $n(\mathbf{r}) = 2 \sum_\eta \{|u_\eta(\mathbf{r})|^2 f(E_\eta) + |v_\eta(\mathbf{r})|^2 [1 - f(E_\eta)]\}$ so that $\int d\mathbf{r} n(\mathbf{r}) = N$. Here $f(x) = 1 / (e^{x/k_B T} + 1)$ is the Fermi distribution function and N is the number of total atoms. Numerically one has to truncate the summation over the energy levels. In practice, we develop a *hybrid* procedure by introducing a high energy cut-off E_c , above which we use a local density approximation (LDA) for the high-lying modes. Thus the regularization prescription (1) leads naturally to an effective coupling constant in the self-consistency equation $\Delta(\mathbf{r}) = g_{eff}(\mathbf{r}) \sum_\eta u_\eta(\mathbf{r}) v_\eta^*(\mathbf{r}) [1 - 2f(E_\eta)]$, where \sum_η is now restricted to $E_\eta \leq E_c$. Further expression of $g_{eff}(\mathbf{r})$ and the detailed LDA contributions to the particle density will be reported elsewhere. Below E_c , we solve the BdG equations by taking $\Delta(\mathbf{r}) = \Delta(r) e^{-i\kappa\varphi}$, where κ denotes the number of vortex flux quanta. Accordingly, we write, for the normalized modes, $u_\eta(\mathbf{r}) = u_{nm}(r) e^{i(m)\varphi} / \sqrt{2\pi}$ and $v_\eta(\mathbf{r}) = v_{nm}(r) e^{i(m+\kappa)\varphi} / \sqrt{2\pi}$. The BdG equations then decouple into different m sectors and reduce to a matrix diagonalization problem if one expands $u_{nm}(r)$ and $v_{nm}(r)$ in a basis set of 2D harmonic oscillators.

We have performed self-consistent computations for a gas with $N = 1000$ for κ up to 10, and have set $a_{ho} = (\hbar/m\omega)^{1/2}$ and $\hbar\omega$ as the units of length and energy, respectively. In the absence of vortices, an interesting aspect of the 2D mean-field theory is that the density profile is essentially *independent* on the interactions, though

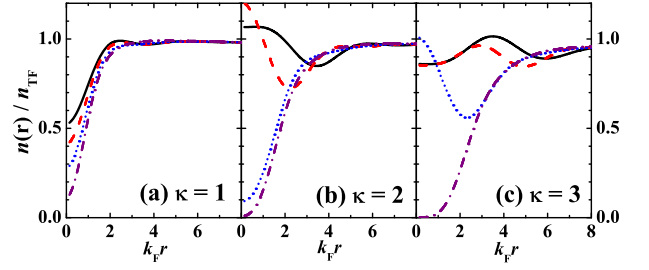


Figure 1: (Color online). Particle density profiles, normalized by $n_{TF} = \sqrt{N}/\pi a_{ho}^{-2}$, for several values of the interaction strengths: $E_a = 0.1E_F$ (solid lines), $E_a = 0.2E_F$ (dashed lines), $E_a = 0.5E_F$ (dotted lines), and $E_a = 2.0E_F$ (dash-dotted lines).

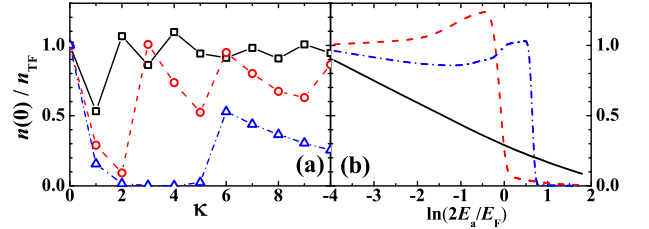


Figure 2: (Color online). Centre particle density as a function of the number of flux quanta (a) and the interaction strengths (b). The symbols in the left panel denote different value of the interaction strengths: $E_a = 0.1E_F$ (BCS side, squares), $E_a = 0.5E_F$ (crossover point, circles), and $E_a = 1.5E_F$ (BEC side, triangles). The lines in the right panel show the results with different number of flux quanta: $\kappa = 1$ (solid line), $\kappa = 2$ (dashed line), and $\kappa = 3$ (dash-dotted line).

the chemical potential is appreciably reduced. Within LDA we find that $n(\mathbf{r})_{\kappa=0} = (\sqrt{N}/\pi)(1 - r^2/r_{TF}^2)a_{ho}^{-2}$ with $r_{TF} = \sqrt{2}N^{1/4}a_{ho}$, and $\mu_{\kappa=0} = E_F - E_a/2$, where $E_F = \sqrt{N}\hbar\omega \equiv k_B T_F$. The resulting maximum value of the order parameter is $\Delta_0 = (2E_a/E_F)^{1/2} E_F$. We have chosen $E_c \simeq 4E_F$, which is already sufficient large to ensure the cut-off independence of our results. The characteristic length scale of the core size of giant vortices is $\xi_\kappa \simeq \kappa\xi$, where the coherence length $\xi \simeq \hbar v_F / \pi \Delta_0 \sim k_F^{-1} = \sqrt{1/2}N^{-1/4}a_{ho}$ in the BCS-BEC crossover regime.

Our main results are summarized in Figs. 1 and 2 where we report the vortex particle density profiles and centre particle densities for several values of the number of flux quanta and the interaction strengths at nearly zero temperature $T = 0.01T_F$. The most unexpected feature of these profiles is the prominent oscillation behavior in the region of the vortex axis for giant vortices with $\kappa \geq 2$, in sharp contrast to the monotonic depletion of the particle density in case of a singly quantized vortex as shown in Fig. 1a. In addition, the centre particle density oscillates with κ and displays a non-monotonic dependence on the interactions. The oscillations in the density profile are

most pronounced on the BCS side and at large number of flux quanta. However, they get suppressed appreciably with increasing the interaction strengths. Nevertheless, they are clearly visible around the crossover regime, and should be easily detected by the absorption imaging in experiments. For a given interaction strength, there is a critical value of the number of flux quanta required to exhibit the oscillations, which increases as the interaction increases. In the nearly BEC regime at $E_a = 1.5E_F$, the oscillation occurs for $\kappa \geq 6$ only, as displayed by the triangles in Fig. 2a. We thus expect that in the extreme BEC limit, these oscillation patterns in the density profiles of all giant vortices should vanish identically, in accordance with the general picture of a fully condensed BEC.

The appearance of the intriguing oscillations in the particle density profile for giant vortices is in close connection to the multiple branches of CdGM bound states inside the vortex core [17]. In the weak coupling limit, a simple semiclassical treatment of the CdGM states leads to a linear spectrum [12],

$$\epsilon_{nm} = \left(n + \frac{1}{2} - \frac{\kappa}{2}\right)E_{\kappa 0} + \left(m + \frac{\kappa}{2}\right)\kappa E_{\kappa 1}, \quad (3)$$

where m is the angular momentum, and the branch index n may take κ integrate values, *i.e.*, from $-\kappa/2$ to $(\kappa - 1)/2$, according to the index theorem established by Volovik for the number of anomalous branches of low-energy quasiparticles inside the core [23]. $E_{\kappa 0} = \pi\hbar v_F/(2\xi_\kappa) \sim 2\Delta_0/\kappa$ and $E_{\kappa 1} = \hbar^2/(2m\xi_\kappa^2) \sim (\Delta_0^2/E_F)/\kappa^2$ are the bound state level spacings [12].

To illustrate the relation between CdGM states and our results on the particle density profiles, we calculate the LDOS $N(\mathbf{r}, E)$, given by $2 \sum_\eta [|u_\eta(\mathbf{r})|^2 \delta(E - E_\eta) + |v_\eta(\mathbf{r})|^2 \delta(E + E_\eta)]$, which, when integrated over negative energy, gives rise to the density profiles $n(\mathbf{r})$. The CdGM states would exhibit themselves as peaks in the LDOS. As the radial functions behave as $u_{nm}(r) \sim r^{|m+\kappa/2|}$ and $v_{nm}(r) \sim r^{|m-\kappa/2|}$ close to the origin, the quasiparticle probability amplitudes $|u(\mathbf{r})|^2$ and $|v(\mathbf{r})|^2$ have maxima at $r \simeq |m|/k_F$ because of the angular momentum of the states [10]. Therefore, the principal contribution to the LDOS at given (\mathbf{r}, E) arises from the bound states with $(|m|, \epsilon_{nm}) = (k_F r, E)$ [10].

Let us first focus on the centre particle density with $m \sim 0$. Fig. 3 shows the LDOS at the vortex axis for different values of the interactions. On the BCS side, where $E_{\kappa 0} \gg E_{\kappa 1}$ (see, *i.e.*, Fig. 3a), there are peaks located both below and above the Fermi surface of $E = 0$ for $\kappa \geq 2$, and their weights may change periodically as a function of κ . As a result, the centre density oscillates with the number of flux quanta. With increasing the interactions, however, the level spacing $E_{\kappa 1}$ becomes progressively larger due to the enhancement of Δ_0 , and therefore $E_{\kappa 0} < E_{\kappa 1}$ across the crossover point. Hence, the interaction turns to expel the bound states towards

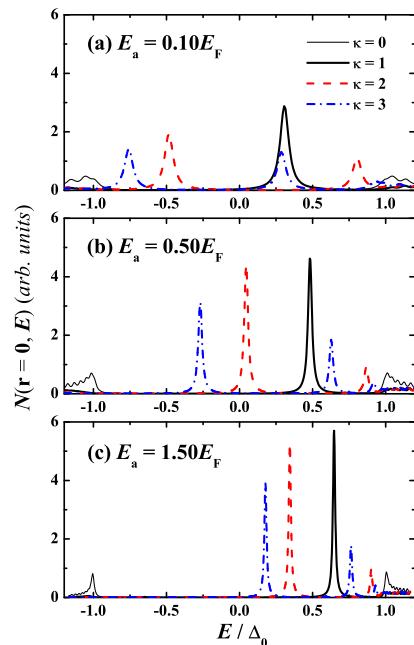


Figure 3: (Color online). Local fermionic density of states at the vortex axis for (a) $E_a = 0.1E_F$, (b) $E_a = 0.5E_F$, (c) and $E_a = 1.5E_F$.

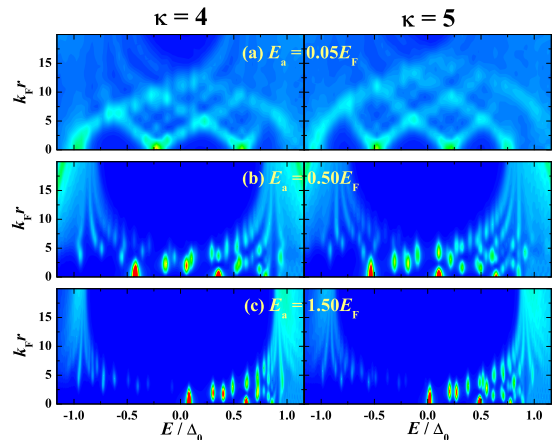


Figure 4: (Color online). Spatial variations of the local density of states for $\kappa = 4$ and $\kappa = 5$ at several values of the interaction strengths as labeled.

the positive energy side. This results a sudden drop of the centre density at a critical coupling strength once the lowest bound state shifts up across $E = 0$, as shown in Fig. 2b. The value of the critical coupling increases with the number of flux quanta.

We now consider the oscillations in the particle density profiles of giant vortices, which may be understood from the spatial dependence of the LDOS, as displayed in Fig. 4 for $\kappa = 4$ and $\kappa = 5$. In the weak coupling limit, the κ branch spectra of CdGM states are quasi-continuous. It

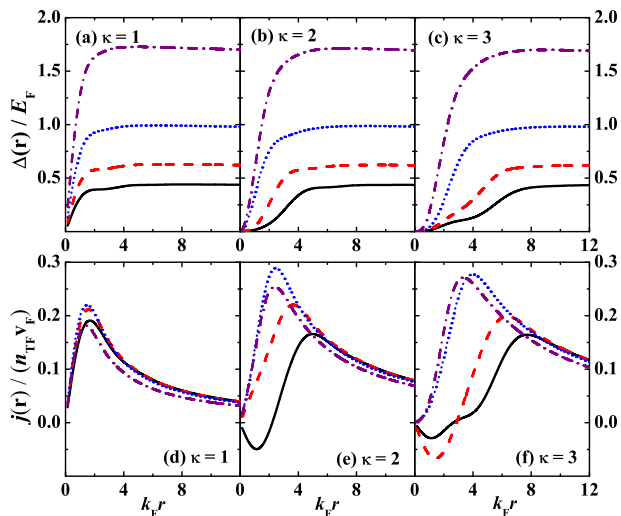


Figure 5: (Color online). Order parameter profiles and current distributions at the vortex core for several values of the interaction strengths: $E_a = 0.1E_F$ (solid lines), $E_a = 0.2E_F$ (dashed lines), $E_a = 0.5E_F$ (dotted lines), and $E_a = 1.5E_F$ (dash-dotted lines). The currents are in units of $n_{TF} v_F$, where $v_F = \hbar k_F / m$ is the Fermi velocity.

is easy to see from Eq. (3) that a wedge-shaped pattern of maxima in the LDOS is formed [10, 11], as shown in Fig. 4a. There are κ rows of peaks as one moves away from the vortex axis, with decreasing number of peaks one by one due to the increase of the angular momentum m . Therefore, the integration over the negative energy of the LDOS naturally yields the oscillation behavior of the density profiles. However, as noted above, the increase of the interaction will make the CdGM states more discrete, with a larger level spacing. This destroys gradually the regular pattern of maxima in the LDOS and the resulting oscillations in the density profile. For a sufficient attraction, see, *i.e.*, Fig. 4c, the LDOS exhausts at the negative energy, and therefore the density profile of giant vortices depletes completely inside the core, resembling that of an ideal BEC as expected.

Finally, in Fig. 5 we report the order parameter profiles and the current circulating around the vortex core. Formally the current density is given by $\mathbf{j}(\mathbf{r}) = (2i\hbar/mr) \sum_{\eta} v_{\eta} \partial_{\varphi} v_{\eta}^* f(-E_{\eta}) \hat{\varphi}$. The order parameter inside the core expands as the flux quanta increases, in accordance with the asymptotic Ginzburg-Landau form $\Delta(r) \sim r^{\kappa}$ ($r \lesssim \xi_{\kappa}$), and enhances with increasing the strength interactions. On the other hand, the current density exhibits a similar oscillation behavior as the particle density for weak interactions. These oscillations are attributed to the interplay between the paramagnetic bound states and the diamagnetic scattering states, which give the opposite contributions to the current, as discussed in Ref. [24] for a two-quantum vortex.

We so far confine to the 2D geometry. By allowing a

free motion of atoms in a box of length L in z axis, we have also studied the 3D situation for a strongly interacting gas of $N = 10^4$ atoms in a cylinder with $L \sim \sqrt{r_{TF}}$, and have observed qualitatively the same features.

In conclusion, by self-consistently solving the mean-field Bogoliubov-de Gennes equations we have analyzed the structure of giant vortices in a superfluid atomic Fermi gas in the strongly interacting BCS-BEC crossover regime. The multiple branches of the CdGM bound states are shown to have a significant impact on the local density of states, and consequently lead to nontrivial oscillations in the giant vortex density profiles. These distinct oscillations, which could be visualized after expanding the cloud, can make a useful diagnosis of giant vortices in atomic Fermi gases.

We acknowledge fruitful discussions with Professor Peter D. Drummond. This work was financially supported by the Australian Research Council Center of Excellence and by the National Science Foundation of China under Grant No. NSFC-10574080 and the National Fundamental Research Program under Grant No. 2006CB921404.

-
- [1] M. W. Zwierlein *et al.*, Nature (London) **435**, 1047 (2005).
 - [2] N. Hayashi, M. Ichioka, and K. Machida, J. Phys. Soc. Jpn. **67**, 3368 (1998).
 - [3] G. M. Bruun and L. Viverit, Phys. Rev. A **64**, 063606 (2001).
 - [4] N. Nygaard *et al.*, Phys. Rev. Lett. **90**, 210402 (2003).
 - [5] A. Bulgac and Y. Yu, Phys. Rev. Lett. **91**, 190404 (2003).
 - [6] J. Tempere, M. Wouters, and J. T. Devreese, Phys. Rev. A **71**, 033631 (2005).
 - [7] M. Machida and T. Koyama, Phys. Rev. Lett. **94**, 140401 (2005).
 - [8] C.-C. Chien *et al.*, Phys. Rev. A **73**, 041603(R) (2006).
 - [9] R. Sensarma, M. Randeria, and T.-L. Ho, Phys. Rev. Lett. **96**, 090403 (2006).
 - [10] S. M. M. Virtanen and M. M. Salomaa, Phys. Rev. B **60**, 14581 (1999).
 - [11] K. Tanaka, I. Robel, and B. Jankó, Proc. Nat. Acad. Sci. (USA) **99**, 5233 (2002).
 - [12] K. P. Duncan and B. L. Györfy, Physica C **404**, 153 (2004).
 - [13] T. P. Simula, S. M. M. Virtanen, and M. M. Salomaa, Phys. Rev. A **65**, 033614 (2002).
 - [14] A. L. Fetter, Phys. Rev. A **64**, 063608 (2001).
 - [15] P. Engels *et al.*, Phys. Rev. Lett. **90**, 170405 (2003).
 - [16] A. Kanda *et al.*, Phys. Rev. Lett. **93**, 257002 (2004).
 - [17] C. Caroli, P. G. de Gennes, and J. Matricon, Phys. Lett. **9**, 307 (1964).
 - [18] X.-J. Liu and H. Hu, Phys. Rev. A **72**, 063613 (2005).
 - [19] D. S. Petrov, M. A. Baranov, and G. V. Shlyapnikov, Phys. Rev. A **67**, 031601(R) (2003).
 - [20] M. Randeria, J.-M. Duan, and L.-Y. Shieh, Phys. Rev. Lett. **62**, 981 (1989).
 - [21] In 3D the maximum value of the circulating current of the singly quantized vortices, j_{max} , shows a non-monotonic

- behavior as a function of $1/(k_F a_{sc})$, peaking at unitarity [9]. Here we find the same dependence of j_{max} on E_a/E_F . Thus we locate the crossover point as the peak position of j_{max} and obtain $E_a \simeq 0.5E_F$.
- [22] F. Gygi and M. Schlüter, Phys. Rev. B **43**, 7609 (1991).
- [23] G. E. Volovik, JETP Lett. **57**, 244 (1993).
- [24] D. Rainer, J. A. Sauls, and D. Waxman, Phys. Rev. B **54**, 10094 (1996).